Annals of Phytomedicine 11(2): 689-702, 2022

DOI: http://dx.doi.org/10.54085/ap.2022.11.2.85

Annals of Phytomedicine: An International Journal

http://www.ukaazpublications.com/publications/index.php

Print ISSN : 2278-9839 Online ISSN : 2393-9885

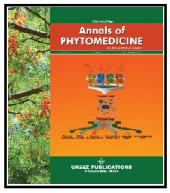

Original Article : Open Access

Ranolazine loaded solid lipid nanoparticles for oral delivery: Characterization, pharmacokinetic and pharmacodynamic evaluation

Abdul Sayeed Khan◆ and Bhupen Chandra Behera*

Department of Pharmaceutics, The Pharmaceutical College, Barpali, Bargarh-768029, Odisha, India

** Department of Pharmaceutics, Kanak Manjari Institute of Pharmaceutical Sciences, Rourkela-769015, Odisha, India*

Article Info

Article history

Received 17 September 2022

Revised 17 November 2022

Accepted 18 November 2022

Published Online 30 December-2022

Keywords

Solid lipid nanoparticles

Ranolazine

Central composite design

Bioavailability

Hot homogenization

Ultra-sonication

Abstract

The antihypertensive and heart-failure drug ranolazine, it is not very soluble in water and does not absorb well in the mouth, thus it is not very useful as a medicine. To boost its oral bioavailability, our study created Ranolazine-loaded solid lipid nanoparticles (Ranolazine-SLNs). Using design of experiments principles, we synthesized ranolazine - SLNs by a hot homogenization and ultra-sonication process. The formulation variables of lipid X1 (glyceryl monostearate), surfactant X2 (Tween 80), and sonication duration X3 were optimized using a central composite design. All of the solid lipid nanoparticle formulations developed had nanometre-sized, spherical particles with high absolute values of zeta potential, indicating excellent long-term stability. The Ranolazine-SLNs studied *in vitro* showed a regulated release profile lasting for at least 24 h. Drug release from the solid lipid nanoparticles was revealed to be much greater than drug suspension *via* studies using dialysis sacs, stomachs, and intestinal tissues from rats. The relative bioavailability of Ranolazine-SLNs was found to be almost 2.3 times that of the commercially available formulation, with a max of 3.9463.95 ng/ml, an AUC of 84.7062.31 ng/ml, and a higher AUC. Based on these findings, Ranolazine-SLNs are a promising new approach to treating hypertension due to their improved bioavailability and positive therapeutic effects. Therefore, these solid lipid nanoparticles may provide a promising alternative to the standard oral formulation for the management of hypertension.

1. Introduction

The therapeutic effectiveness of a medicine is determined by how well it is absorbed, distributed, metabolized, and excreted inside the body. Treatment failure may occur when a medicine is not present in the body at a high enough concentration because of poor absorption, quick metabolism and elimination, poor drug solubility, or large fluctuations in plasma levels caused by unexpected bioavailability. The creation of an effective medication colloidal carrier system is a viable approach to overcoming these challenges. There are several benefits to using solid lipid nanoparticles as a colloidal carrier system, and just a few drawbacks. With their biodegradable, biocompatible, and low-toxic qualities, solid lipid nanoparticles (SLN) have received interest as carriers for the synthesis of a broad range of poorly water-soluble medicines (Delic *et al.*, 2020).

The use of SLNs as an alternative to polymeric nanoparticles in the delivery of drugs has been described (Muhlen *et al.*, 2005). Solid-lipid nanoparticles (SLNs) have an advantage over polymeric nanoparticles due to their lipid matrix, which is composed of physiologically acceptable lipid components, and therefore reduces the risk of both acute and chronic toxicity (Mehnert *et al.*, 2001). The particles remained in a solid form even when cooled to room temperature (Mehnert *et al.*, 2001). SLNs have the potential to combine the benefits of polymeric nanoparticles, fat emulsions, and liposomes (Veerendra and Yeligar *et al.*, 2021), *i.e.*, controlled release like polymeric nanoparticles, high-volume synthesis, and low toxicity. There have been reports of SLNs being used to control drug delivery, increase the bioavailability of entrapped pharmaceuticals by the adjustment of dissolution rate, and/or improve tissue distribution and targeting of medications (Tiwari *et al.*, 2022). There have been no published papers detailing the influence of SLNs on pharmacodynamics as of yet.

Newer novel antianginal drug ranolazine, with its anti-ischemic and metabolic effects, was first licensed by the US FDA in 2006 for the treatment of patients with angina pectoris. The effective dosage of the extended-release version of ranolazine is 500 to 1000 mg twice day and its half-life is 1.4 to 1.9 h (Torsten *et al.*, 2005). The downsides of the currently available ranolazine formulation include hepatic first pass metabolism, poor absorption, decreased bioavailability, high dosage, and gastrointestinal side effects. Therefore, treating angina pectoris using an unique carrier drug delivery system that allows for reduced medication dosage, avoidance of first pass effect, higher bioavailability, regulated drug administration, and overall patient compliance would be an excellent option. Thus, lipid nanoparticles, a new vesicular drug delivery method, were chosen for ranolazine's systemic drug administration (Tardif *et al.*, 2005).

The purpose of this study was to find a way to increase the oral bioavailability of ranolazine by incorporating it into triglycerides so that solid lipid matrices could be created and the intestinal lymphatic transport could be used. In addition, pharmacodynamic studies of Ranolazine-SLNs in animal models are being conducted. So, we used

Corresponding author: Mr. Abdul Sayeed Khan

Associate Professor, Department of Pharmaceutics, The Pharmaceutical College, Barpali, Bargarh-768029, Odisha, India

E-mail: sayeed78khan@gmail.com

Tel.: +91-9090570021

the heat homogenization and ultrasonication procedure to get the Ranolazine-SLNs ready (Tardif *et al.*, 2005). In fructose-induced hypertensive wistar rats, we compared the effects of a suspension of ranolazine to those of a prepared SLN on pharmacokinetics and pharmacodynamics.

2. Materials and Methods

2.1 Materials

Alembic Pharmaceutical Limited, an Indian pharmaceutical firm, provided us with a free trial sample of ranolazine. The 500 mg ranolaz tablet was acquired from the drug store. The glyceryl monostearate lipid sample from SD Fine Chemicals, India. Both Poloxamer 188 and Poloxamer 407 from BASF, Mumbai. The rest of the compounds utilized were all of an analytical grade (Chaitman *et al.*, 2005; Sayed *et al.*, 2007, Kumar *et al.*, 2015, Paolino *et al.*, 2005; Jun-Bo *et al.*, 2007).

2.2 Methods

2.2.1 Solubility study

It is important to pick a lipid in which the medicine is maximally soluble in order to construct an SLN. Each lipid had 100 mg melted at 5ºC over its melting point. A total of 100 mg of medication was gently added to each lipid until supersaturation was reached. Drug solubility in lipids was evaluated (Pamer *et al.*, 2011; Imad *et al.*, 2020).

2.2.2 Formulation of Ranolazine-loaded SLNs

The SLNs loaded with ranolazine were made using the heat homogenization process, with a lipid of 5-10% w/v glyceryl monostearate (Imwitor 491/GMS) and a surfactant of 1-3% w/v pluronic P407: tween 80 (1:1 w/w). To create the medicine lipid melt, GMS was heated to 5ºC above its melting point, and then ranolazine was added and thoroughly dissolved. They used distilled water and surfactant to make an aqueous surfactant solution at the same temperature. While continuously stirring to maintain temperature, the resulting hot aqueous phase was added to the drug lipid melt to create a coarse pre-emulsion. After forming an o/w emulsion using an ultra-turrax high-speed homogenizer spinning at 14,000 rpm for 15 min, the mixture was heated and sonicated using a probe. The mixture was kept in airtight glass bottles after being cooled to room temperature to solidify the nanoparticles into SLNs. The SLNS were lyophilized with the use of a lyoprotectant called trehalose (1:4 w/w) (Heto dry winner, Denmark). Samples were lyophilized and kept at 2-8ºC until further use (Vasudha *et al.*, 2022; Dandamudi *et al.*, 2022).

2.2.3 Optimization of SLNs formulation using central composite design (CCD)

Optimizing the important formulation factors and quantifying the relationship between them using CCD. Design-expert® 12.0.3.0 software for a two-component system was used to create the CCD and carry out the optimization analysis. These kinds of research sometimes need a large number of trials, the exact amount of which is proportional to the number of independent variables being tested. The quantity of lipid, the concentration of the surfactant, and the duration of the sonication are the three variables in this design. The % entrapment efficiency YI variable, particle size Y2 and Y3 variables, and zeta potential Y4 variables were chosen as the dependent variables (Table 1). Since particle size (in nm) and entrapment efficiency (in %) are so important to formulation performance and drug usage, they were taken into account as response factors (Carvalho *et al.*, 2013; Varshosaz *et al.*, 2010; Weon *et al.*, 2000). The program generated 20 tests with 5 fixed points each. Predictions about how changing the independent variables would affect the response parameters might be drawn from the corresponding response surface plots.

$$Y = b0 + b1X1 + b2X2 + b3X3 + b12X1X2 + b13X1X3 + b23X2X3+b11X12+B22X22B33X32$$

where Y represents the response to each factor level combination (in terms of particle size, EE, PDI, and zeta-potential for the formulation variables), b0 is an intercept, and bl to b33 are regression coefficients for corresponding variables.

Table 1: Factors used in experimental design

Independent variables			
Parameter	**Low (-1)**	**Medium (0)**	**High (+1)**
X1 (%w/v)	5	8	10
X2 (%w/v)	1	2	3
X3 (min)	5	75	10
Dependent variables			
Y1 (%)		Maximize	
Y2 (nm)		Minimize	
Y3		In range	
Y4		Maximize	

2.3 Characterization of Ranolazine-loaded SLNs

2.3.1 Entrapment efficiency

Centrifugation was used to calculate the trapping effectiveness of SLN dispersion (Luo *et al.*, 2006). An SLN suspension was spun at 20,000 rpm for one hour in a cold centrifuge to separate the supernatant liquid. Following appropriate dilution with a new phosphate buffer saline pH 7.4, the recovered liquid was filtered to quantify the free drug concentration. A UV spectrophotometer was used to detect absorbance at 272 nm (Chettupalli *et al.*, 2021), and the entrapment efficiency was derived using the following formula:

Entrapment efficiency = Wt. of drug incorporated/Wt. of drug initially taken × 100

2.3.2 Measurement of particle size, PDI and zeta potential of SLN

Using a zetasizer, we determined the SLNs' size, polydispersity index, and zeta potential (ZP) (Nano ZS90, Malvern, Worcestershire, UK). To get an optimal kilo counts per second (Kcps) of 50-200 for measurements (Amarachinta *et al.*, 2021), 100 l of the produced SLN dispersion was diluted to 5 ml with double distilled water.

2.3.3 Determination of total drug content

Dissolving the SLNs formulation in a chloroform:methanol (1 : 1) combination and then diluting it further with mobile phase yielded a final volume of around 100 l. Amounts of ranolazine in formulations were determined by injecting diluted samples onto an HPLC column (Manjunath *et al.*, 2005).

2.3.4 *In vitro* drug release studies

The dialysis technique was used to study release *in vitro*. The release investigations made use of a dialysis membrane (Himedia, Mumbai, India) with a molecular weight cut-off of 12,000-14,000 daltons. The dialysis membranes were pre-soaked in a solution of double-distilled water for a whole night before the release tests were performed. The releasing media were 0.1 N hydrochloric acid and a phosphate buffer at pH 6.8. Donor and receiver cells were separated in the experimental unit. For the release investigation, 1 ml of the SLNs dispersion was transferred into a boiling tube with a dialysis membrane connected to one end. A 250 ml beaker containing 100 ml of release media served as the receptor compartment, which was kept at 37 0.5°C. Samples of 2 ml were taken from the receiver compartment and replaced with the same amount of release medium at 0, 0.25, 0.5, 1, 2, 3, 4, 6, 8, 10, 12, and 24 h. Following appropriate dilution, the obtained samples were examined at 274 nm (Pradhan *et al*., 2011) using a UV-Visible spectrophotometer (SL-150, ELICO, Hyderabad, India).

2.3.5 Stability study

Lyophilized samples of optimized ranolazine-SLNs packaged in air-tight glass vials were subjected to stability testing by being kept in a stability chamber (Remi, Mumbai, India) for three months at RT 25 2 C, relative humidity (RH) of 60 5%. At the end of each month throughout the three-month storage period, samples were taken and analyzed for particle size, PDI, zeta potential, LE%, and *in vitro* release behavior. Each month's worth of data was compared to those of newly manufactured Ranolazine-SLNs (time zero sample). Triplicates were used in the stability tests (Attari *et al*., 2016).

2.3.6 *Ex vivo* diffusion study

Male wistar rats weighing about 200-250 g were chosen and fasted overnight to ensure their health. After euthanizing the rats humanely, we removed their intestines and cleaned the separated stomach and duodenum with cold Krebs ringer's solution to eliminate any mucus or lumen contents. After the open end of the stomach and duodenal tissue was tied off, the formulation (drug suspension and ranolazine-loaded SLNs) was inserted. After making sure, there was no leak at the other open end, we tied it off securely. To continue the research, 100 ml of 0.1N HCl (containing 1% SLS) was administered to the stomach, and 100 ml of PBS pH 6.8 (containing 1% SLS) was administered to the duodenum. The whole experiment was conducted with a constant supply of carbogen and mild stirring at 37 2°C. In the stomach, 1 ml aliquots were taken every 2 h and in the duodenum, every 8 h, with the old media being discarded and the new media being added before the samples were examined using UV-visible spectrophotometry (Unnisa *et al*., 2022; Smith,1996).

2.3.7 Lyophilization of SLNS

The stability of SLNs was improved by lyophilization. The SLNs were made using 10% w/v maltose and stored overnight at 40°C (Sanyo, Tokyo, Japan). Freeze-dryers were used on the frozen samples (Lyodel, Delvac Pumps Pvt. Ltd, Chennai, India). After applying vacuum and through several drying processes for around 48 h, a powdered lyophilized product was obtained (Cavalli, 1997).

3. Solid state characterization

3.1 Drug-excipient compatibility studies by differential scanning calorimeter (DSC)

Using Universal V4 TA equipment from Chicago, IL, USA, DSC analysis was done on ranolazine, GMs, tween 80, Poloxamer 188, physical mixtures (PM in 1:1 ratio), and lyophilized Ranolazine-SLNs. Indium was used in the instrument's calibration. Dry nitrogen was used as the effluent gas, and aluminum pans held all of the samples (10 mg). The experiment was conducted at a heating rate of 20°C/min and a temperature range of 20-200°C (Arjun *et al*., 2013; Vinay *et al*., 2007).

3.1.1 Morphology by scanning electron microscopy (SEM)

Scanning electron microscopy was used to investigate nanoparticle morphology (SEM, Hitachi, Tokyo, Japan). A drop of nanoparticle formulation containing freeze-dried solid lipid nanoparticles of ranolazine was put on a sample holder and allowed to air-dry. The sample was then seen at an accelerating voltage of 15.000 volts while under a variety of magnifications. This imaging was performed in a very tight vacuum (Vijayakumar *et al*., 2009).

3.1.2 Morphology by transmission electron microscopy (TEM)

Freeze-dried Ranolazine-SLNs were negatively stained with a sodium **phosphotung** state solution (0.2% w/v), and then seen under a transmission electron microscope (TEM) to determine their morphology (Madhu *et al*., 2013). The carbon-coated copper grid had a drop of SLN dispersion placed on it to create a thin coating. A drop of the phosphotungstic acid staining solution was applied to the film before it was dried on the grid, and any excess solution was drained off using filter paper. After letting the grid dry naturally, samples were examined using a TEM (JEOL-100CX-II, Tokyo, Japan).

3.2 Bioavailability study

3.2.1 Study design and sampling schedule

Wistar rats were used in a single-dose bioavailability study while they fasted. By administering a dosage of 10 mg/kg of body weight orally to wistar rats, researchers were able to evaluate the oral bioavailability of the improved SLNs formulation and drug solution. Kakatiya University's College of Pharmaceutical Sciences Institutional Animal Ethics Committee gave its stamp of approval to all experiments before they were conducted (Warangal, India). For this investigation, wistar rats weighing between 200 and 250 g were culled (6 animals per group). Retro-orbital venous plexus punctures were performed to collect blood samples at 0, 0.5, 1, 1.5, 2, 3, 4, 6, 8, 10, 12, and 24 h after dosing. Blood samples (about 15 ml) were collected in Eppendorf tubes and centrifuged at 3000 rpm for 30 minutes. The serum was then placed in a different Eppendorf tube and frozen at 20°C in preparation for analysis.

3.2.2 HPLC analysis

At a flow rate of 1 ml/min, a combination of methanol, 20 mM potassium dihydrogen phosphate (pH 4.5), and triethanolamine (70:30:0.2 v: v) was used to equilibrate a Merck C18 (250 4.6 mm) HPLC column. Without interference from serum, the peaks eluted at 254 nm (Ashok *et al*., 2010). The linearity range for Ranolazine was determined to be 50-5000 ng/ml, with a r^2 of 0.996, the LOD being 20 ng/ml, and the LOQ being 50 ng/ml.

3.2.3 Extraction procedure

Serum was diluted to 0.1 ml with the addition of 0.1 ml of the internal standard irbesartan (3 g/ml) and 0.4 ml of acetonitrile. The solutions were centrifuged at 5000 rpm for 25 min in an Eltek, Model TC 650 D, Mumbai, India, vortex mixer for 2 min. The liquid in the top phase was evaporated in a nitrogen evaporator after being filtered using a 0.45 filter. After reconstituting the extracted material in mobile phase, 20 l of ultra-filtrate was injected. Ranolazine had a 7.6 min retention time, whereas the internal standard had a 3.8 min retention time.

3.2.4 Estimation of pharmacokinetic parameters and statistical significance

Kinetica was used to determine pharmacokinetic parameters such as maximum serum concentration (Cmax), time to reach Cmax (tmax), area under the concentration-time curve (AUC), biological half-life (t1/2), and mean residence time (MRT) (version 5.0). Statistical dispersion was used to express the data. Two samples were compared using an unpaired student *t*-test in Graph Pad Prism (version 6.02.2013), and a significance level of $p<0.01$ was accepted.

3.3 Pharmacodynamic study

Wistar rats of the male species weighing 210-250 g were employed, with full access to food and water. Water from the faucet or a 10% fructose solution was used as the drinking fluid (Hwang *et al*., 1987). The rats were conditioned to maintain a relaxed and subdued demeanor in the rat holder during the whole BP measurement process. After two weeks, we chose rats with mean systolic blood pressures of at least 140-145 mm Hg. Each of the three groups, A, B, and C, included six hypertensive rat pups. The control group (group C) got no treatment, whereas groups A and B each. received 10 mg/kg of the medication orally in the form of a suspension (SLNs formulation and suspension, respectively) (Bhasker *et al*., 2009). Systolic blood pressure was recorded for normal rats using the tail- cuff technique (NIBP. IITC, CA, USA) at various time intervals (0, 1, 2, 4, 6, 12, 24, 36, 48, and 60 h) (group D).

3.3.1 Tail-cuff method

Systolic blood pressure and heart rate were monitored in rats using the tail-cuff technique at a stable room temperature of 33ºC. The rats were housed in plastic pens that were subsequently moved to climate-controlled rooms. The tail was cuffed and a pneumatic pulse sensor was fitted. Two days were given to acclimate the rats to the technique before any tests were run on them. Each rat had at least three consecutive measurements of their systolic blood pressure and heart rate taken on an NIBP, IITC 59/29 model and then averaged.

4. Results

4.1 Solubility study

To prevent medication precipitation from the lipid in formulation, a solubility study was conducted. Figure 1 depicts the solubility of ranolazine in a variety of pharmaceutically approved lipids. Glyceryl monostearate was determined to be the lipid in which the medication was most soluble, and therefore it was chosen as the lipid for the SLNs. Ranolazine was most soluble in glyceryl monostearate (Imwitor 491).

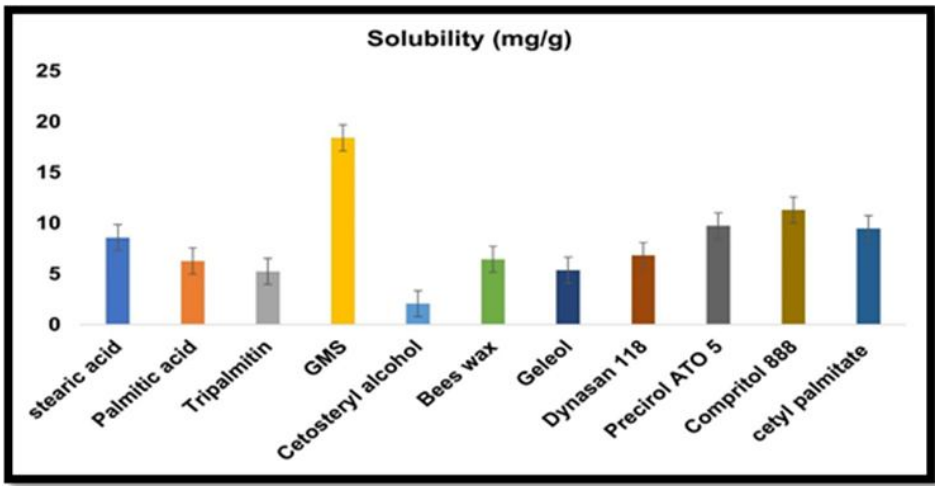

Figure 1: Solubility study of drug in lipid.

4.1.1 Optimization of formulation variables by central composite design

Since entrapment efficiency (EE), particle size (PS), particle distribution index (PDI), and zeta potential are all affected by the amount of lipid (glyceryl monostearate) and the concentration of surfactant (Pluronic P407: Tween 80 1:1 w/w); these two factors were chosen as independent variables after preliminary optimization. Parameter values used in formulation and the overall plan for the composite structure are listed in Table 1. Each batch was fine-tuned to achieve maximum entrapment efficiency (Y1), particle size (Y2), particle distribution index (PDI) (Y3), and zeta potential (Y4) (Y4). After collecting data from each experiment, multiple regression analysis and the F-statistic were used to determine whether the answer best suited the simple linear Eq. (1-4) or the quadratic Eq. (3). As a result of the mathematical modeling, a polynomial equation of the second order was obtained. The quadratic medel with the lowest *p*-value ($p<0.0001$) was chosen as the most appropriate one. Multiple regressions were performed on the PS and EE at different levels of two independent variables (X1, X2, and X3) to get a second order polynomial equation.

Table 2: Results from CCD-based experimentation and resulting values for key parameters formulation of a statistical plan for the generation of spatial link networks

Run	X1	X2	X3	Y1	Y2	Y3	Y4
1	5	1	5	76.35 ± 0.2	235.46 ± 2.68	0.332 ± 0.01	-39.4 ± 2.35
2	7.5	2	7.5	60.37 ± 2.1	198.36 ± 3.45	0.523 ± 0.05	-18.3 ± 1.03
3	7.5	0.31	7.5	92.16 ± 0.6	127.39 ± 1.95	0.046 ± 0.04	-34.2 ± 2.04
4	7.5	3.68	7.5	80.43 ± 1.5	140.23 ± 6.31	0.012 ± 0.03	-20.5 ± 0.68
5	10	1	5	89.35 ± 0.8	134.21 ± 8.21	0.048 ± 0.01	-36.4 ± 1.39
6	7.5	2	7.5	60.34 ± 0.3	200.52 ± 3.49	0.526 ± 0.11	-20.7 ± 2.17
7	10	1	10	88.34 ± 1.2	123.64 ± 7.36	0.095 ± 0.02	-22.5 ± 2.07
8	5	1	10	40.23 ± 1.5	385.21 ± 6.51	0.594 ± 0.13	-25.3 ± 0.59
9	7.5	2	7.5	63.15 ± 3.5	196.35 ± 2.94	0.532 ± 0.01	-18.1 ± 1.26
10	11.7	2	7.5	69.02 ± 2.4	235.46 ± 9.35	0.361 ± 0.15	-25.9 ± 2.43
11	3.29	2	7.5	46.21 ± 0.6	364.21 ± 5.16	0.498 ± 0.03	-30.4 ± 1.35
12	10	3	10	55.31 ± 0.4	110.27 ± 3.84	0.035 ± 0.12	-26.8 ± 0.36
13	10	3	5	54.06 ± 0.7	294.35 ± 2.49	0.312 ± 0.05	-22.4 ± 1.25
14	7.5	2	3.29	80.13 ± 0.5	265.81 ± 6.97	0.305 ± 0.04	-36.8 ± 0.43
15	7.5	2	11.7	52.34 ± 1.3	249.71 ± 7.05	0.225 ± 0.09	-20.4 ± 2.13
16	5	3	5	74.26 ± 2.5	268.38 ± 3.51	0.196 ± 0.07	-26.4 ± 0.46
17	7.5	2	7.5	60.33 ± 3.1	198.36 ± 4.98	0.552 ± 0.03	-18.3 ± 0.22
18	7.5	2	7.5	60.38 ± 0.1	168.43 ± 3.15	0.542 ± 0.04	-23.4 ± 0.58
19	7.5	2	7.5	60.32 ± 0.5	210.35 ± 3.26	0.413 ± 0.01	-14.9 ± 0.37
20	5	3	10	55.02 ± 0.8	203.58 ± 4.62	0.065 ± 0.23	-23.6 ± 0.12

4.1.2 Analysis of entrapment efficiency

The entrapment efficiency (EE) values obtained from the trials ranged from 40.231.5 (formula 8) to 92.160.6%. (formulation 3). Table 4 shows that the %EE was affected by the surfactant concentration and the lipid/surfactant ratio. The relationship between the magnitude of a factor and the percentage of energy expended is described by the following equation:

E = +60.94 +5.83A -5.52B -7.46C -10.13AB +6.95AC +2.39BC -1.97A2 +8.17B2 +1.07C2

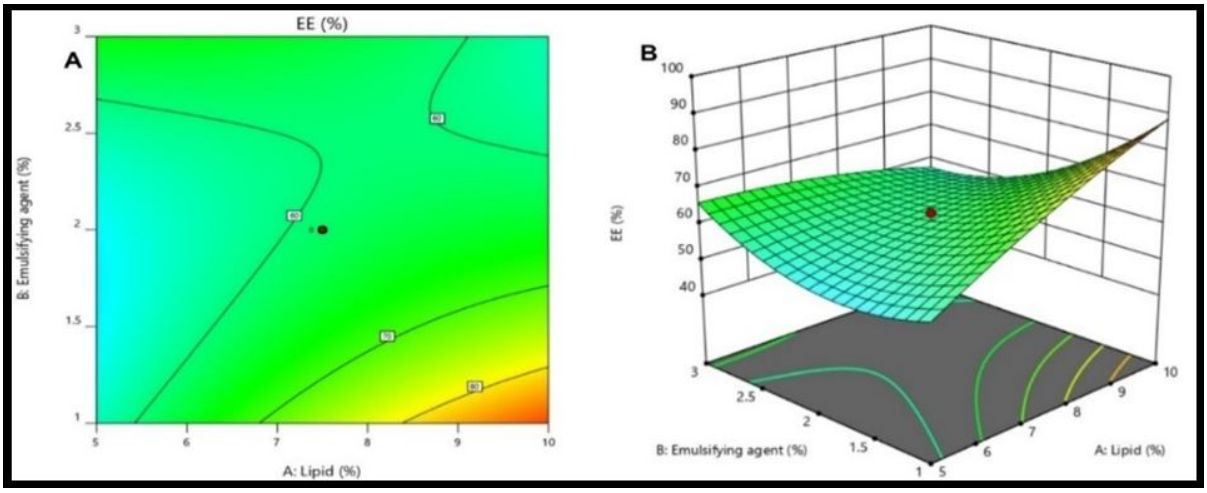

Figure 2: Plots of independent variables vs counter and response-surface plots (EE).

Entrapment efficiency was measured to be between -40.23 (1.5) and -92.16 (0.6) per cent. The model is statistically significant, since the F-value for it, is 31.72. The F-value is high, could only happen by accident 0.01% of the time. When the probability value for the model term is smaller than 0.0500, we say that the term is significant. In this context, the model terms A, B, C, AB, AC, tern and B2 are all important. If, the value is more than 0.1000, then the model terms are not important. Model reduction may be useful, if your model has numerous meaningless words (apart from those needed to maintain hierarchy). Because of its high significance, the lack of fit has an F-value of 20.24. Lack of Fit F-values as big as this one have a 0.25 probability of being attributed to random chance alone. It is not good if there is a drastic mismatch between the data and the model. The 0.7431 predicted R^2 and the 0.9357 adjusted R^2 are not too far off from one another. A measurement of the signal-to-noise ratio is made by Adeq precision. Ideally, the ratio would be higher than 4. With a ratio of 19.853, you have a strong enough signal to proceed.

4.1.3 Effect of independent variables on particle size

The range of Ranolazine-SLN particle size is from 100.13 7.2 to 399.08 2.4 nm. The polynomial equation, three-dimensional graphs, and contour diagrams were all used to illustrate how a given factor affects particle size (Figure 2). The lipid increases the size of SLNs in an agonistic manner. Larger SLNs were seen at higher lipid concentrations (from 5% to 10%). Particles aggregate, leading to particle enlargement. Tween 80, the second component, has a negative effect on particle size; increasing the concentration from 2% to 3% causes the SLN size to decrease. The particles may be smaller because the interfacial tension between the two phases is lower. As sonication progresses, particles get smaller. As sonication duration increased, particles were broken down into smaller and smaller pieces, resulting in smaller and smaller SLNs. Vesicle size = +195.82 -47.35A +1.44B -10.02C +36.94AB -34.95AC -48.51BC +34.14A2-24.56B2 +19.26C2.

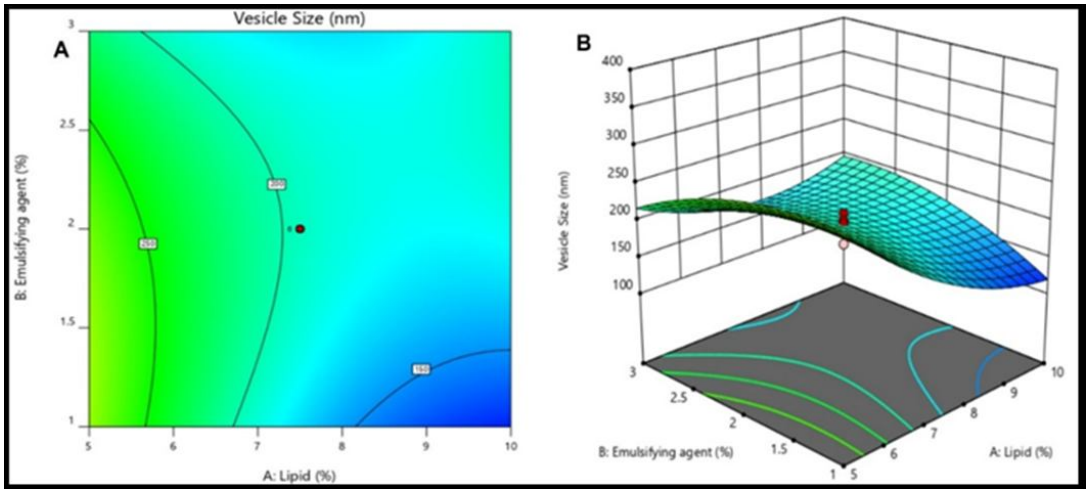

Figure 3: A plot of the influence of the independent factors on particle size is shown on the response surface (Y2).

When the F-value for a model is 40.42, it is statistically significant. The F-value is high, could only happen by accident 0.01% of the time. When the probability value for the model term is smaller than 0.0500, we say that the term is significant. In this context, the model terms A, AB, AC, BC, A2, B2, and C2 are all important. If, the value is more than 0.1000, then the model terms are not important. Model reduction may be useful if your model has numerous meaningless words (apart from those needed to maintain hierarchy). A 1.89 F-value for lack of fit indicates that the lack of fit is not statistically different from random error. A lack of fit F-value as high as this one has a 25.08% likelihood of being related to noise.

The difference between the predicted R^2 of 0.8509 and the adjusted R^2 of 0.9492 is less than 0.2, suggesting that the two measures are consistent with one another. A measurement of the signal-to-noise ratio is made by Adeq precision. Ideally, the ratio would be higher than 4. With a ratio of 21.572. your signal strength is good.

4.1.4 Effect of independent variable on size distribution (PDI)

The use of PDI in the creation of SLNs is also crucial. The PDI chart represents the size distribution of the sample population. For a totally homogeneous sample with regard to particle size, the PDI value would be 0, whereas for a more diverse sample, it would be 1 (for a highly poly disperse sample with multiple particle size populations). In practice, appropriate values for polymer-based nanoparticle materials are often considered to be 0.2 or below. A PDI of 0.3 or below suggests a homogeneous population of phospholipid vesicles, which is desirable in drug delivery applications using lipid-based carriers like liposomes and nano liposome formulations. The criteria for an acceptable PDI are not mentioned in the most recent edition of the FDA's "Guidance for Industry" regarding liposome drug products, despite its emphasis on size and size distribution as "critical quality attributes (CQAS)" and essential components of stability studies of these products. Regulatory agencies should provide more detailed rules and recommendations for the acceptable range of product PDI for various uses (*e.g.*, food, cosmetics, pharmaceuticals, *etc.*) and delivery methods of bioactive substances.

It was preferable that the particles be smaller than 200 nm. Different models were used to match the response data, and it was discovered that the quadratic model was the most appropriate. This model's F-value was 29.67. and the "Prob> F value was less than 0.05, therefore, it was considered statistically significant (p<0.0001).

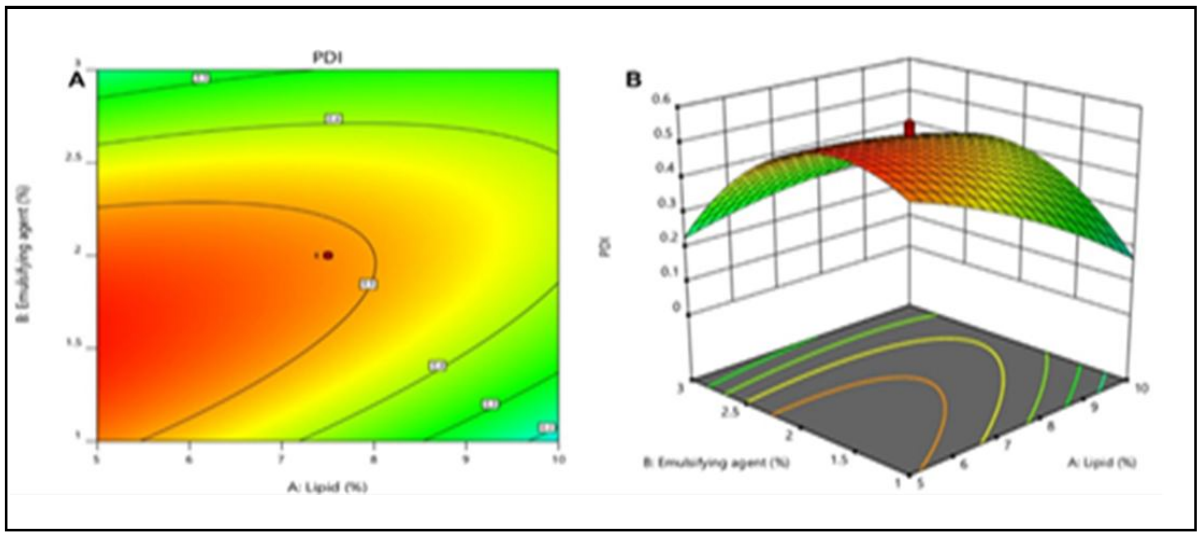

Figure 4: PDI studies using counter and 3D surface response plots.

PDI= +0.5151 -0.0679A -0.0379B -0.0171C +0.1086AB -0.0451AC -0.0896BC -0.0333A2 - 0.1749B2 -0.0914C2

4.1.5 Zeta potential

All formulations had negative ZP values when tested. However, ZP was treated as an absolute value (*i.e.*, without a negative or positive sign) for the purposes of the data analysis that were performed. Results for the ZP of the finished nanoparticles are shown in Table 2. Each factor's influence on the final ZP is shown in Equation 5.

Zeta potential: -18.97 +1.04A 3.47B +3.95C -0.6250AB -9250AC -3.70BC -3.70A2 -2.81B2 - 3.26C2

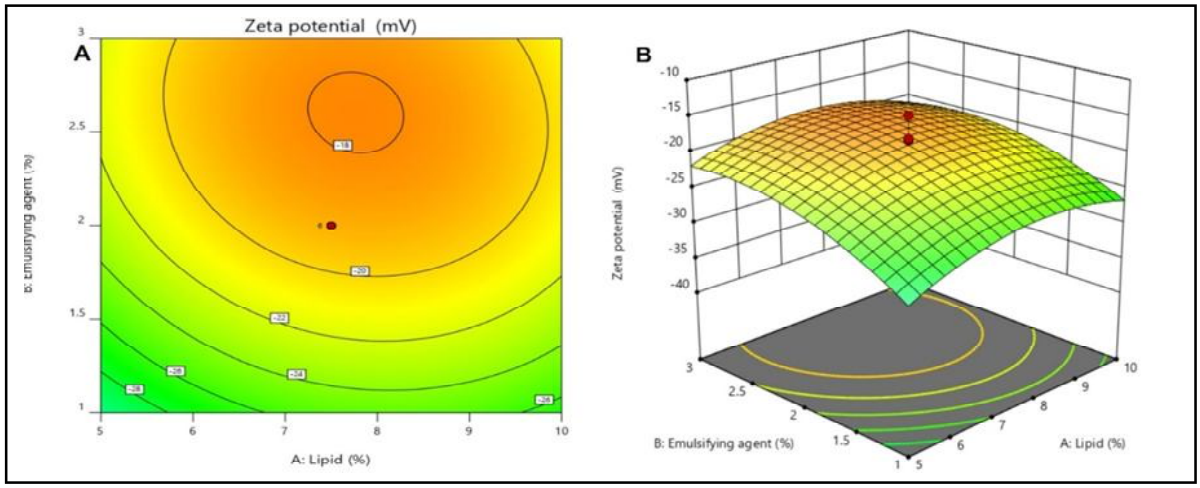

Figure 5: Formulation variables shown as contour plots and three-dimensional surfaces.

4.1.6 Optimization of independent variable and validation

Once the polynomial equations representing the dependent and independent variables had been analyzed, an optimization and validation procedure using design expert software was carried out to investigate the best possible formula solution for SLNs. Maximum EE, minimum particle size, and particle distribution index (PDI) were the normative requirements for this. Optimal formulation was found to include 10% w/w lipid and 1% w/w surfactant, meeting all optimization criteria. At these concentrations, the expected sizes of particles (YI), particle distribution indices (Y2), and effective enthalpies (EE) were 130.864 nm, 87.1359, and 0.145, respectively. Therefore, a fresh batch of SLNs was generated using the optimum formulation factor values in order to verify the projected model. Good agreement was found between the anticipated and actual values of PDI (0.0950.02), particle size (123.647.36 nm), and EE (88.341.2%) for the improved formulation. Consistent with the theoreticalexpectations, our experimental findings support the use of CCD to foretell an optimal SLN formulation.

4.1.7 Measurement of particle size, PDI and zeta potential of SLN

Particle size distribution, zeta potential, and PDI values were all calculated for each of the finished formulations. All the average sizes of the different formulations were between 123.647.36 nm and 385.216.51 nm. The limited size range was reflected by the PDI values of 0.0120.03 to 0.5940.13. The length of the alkyl chains in the triglyceride was correlated with the particle size. When

Ranolazine was included into the SLNs formulations, a negative surface charge was observed, which provided strong evidence for the drug's orientation inside the lipid matrix. For colloidal dispersion to be stable, surface charge plays a crucial role. In our experiments, we discovered that the zeta potential of SLNs formulations ranged from -14.90.37 mV to -39.42.35 mV. As it is, it is accepted that electrostatic stability requires a zeta potential of less than 30 mV. Many investigations, however, showed that the steric stabilizer might also provide stability to the SLNs' dispersion, complementing the electrostatic repulsion. The formulation included Poloxamer 407 as a stabilizing agent. The non-ionic surfactant formed a coating on the SLNs' surface, reducing electrostatic repulsion between the particles after sterically stabilizing them.

4.1.8 Determination of entrapment efficiency and drug content

We calculated the total drug content of the SLNs and found it to be between 97.560.04% and 99.050.01%. A range from 40.231.5% to 92.160.6% was observed for the entrapment efficiency of the SLNs formulations. Ranolazine's strong lipophilicity made it particularly well-suited for encapsulation in triglyceride nanoparticles (Table 2). The glyceride may be able to hold more lipophilic medicines because of the long-chain fatty acids connected to it. A number of drug molecules may be trapped in the less organized lipid matrix due to its flaws and resulting empty spaces. There was no drug leakage or precipitation throughout the preparation process since the medication was dissolved in molten lipid at a temperature above the melting point of the lipid. Drugs that are efficiently encapsulated in lipid nanoparticles are more likely to be delivered to their intended target through lymphatic transport, skipping first-pass digestion in the process solid-state characterization

4.2 Drug-excipient compatibility studies by DSC

DSC was used to probe the lipids' compatibility in the SLNs formulation. Figure 6 displays differential scanning calorimetry (DSC) thermograms of the unadulterated drug, unadulterated lipid, physical mixing of drug and lipid (1:1), and lyophilized SLNs formulation. A high endothermic peak at 151.90°C with -120.42 J/g enthalpy was seen in the DSC thermogram of pure ranolazine, correlating to the drug's 100% crystallinity. At 52.65°C, the emulsifying agent reached its endothermic peak, displaying an enthalpy of -143.82 J/g. It was determined that the drug peak in carbopol occurred at 161.74°C and the lipid peak at 65.83°C, and that the enthalpy values were 487.67 J/g. The crystallinity dropped to 89.34%. Lack of an endotherm peak in lyophilized SLNs formulations provides insight into the drug's amorphization from its natural crystalline state. SLNs were discovered to have a crystallinity of 25.04% and 28.74%, respectively. Previous research has also revealed similar findings.

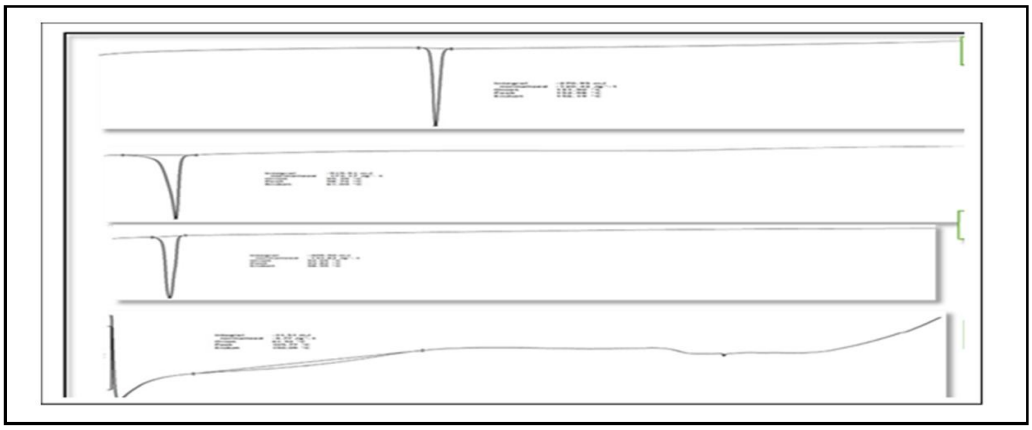

Figure 6: DSC thermogram comparing (from left to right): (A) Pure drug, (B) GMS, (C) Poloxamer 188, (D) Optimized SLNs.

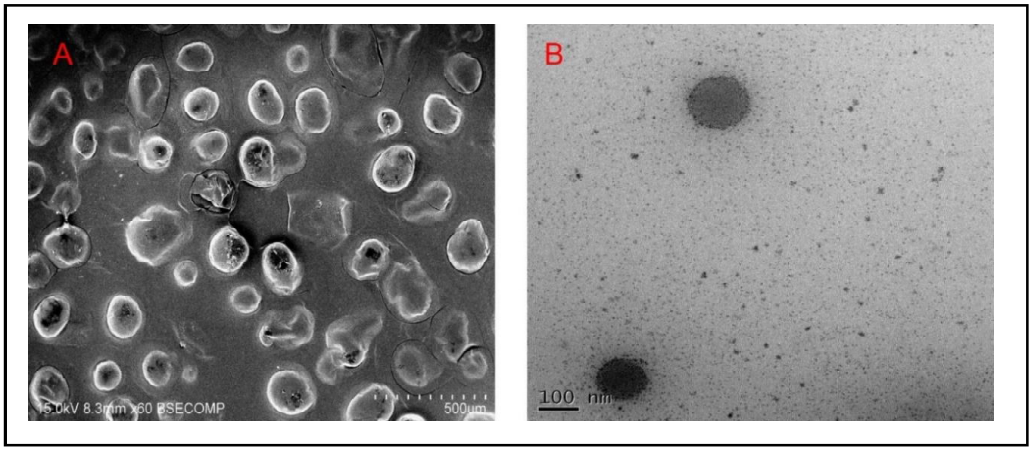

Figure 7: Optimized SLNs formulation A. Scanning electron microscopy and B. transmission electron microscopy morphological studies.

4.2.1 Morphology of SLNs using SEM and TEM

The surface morphology of SLNs formulation was examined by scanning electron microscopy (SEM) at 10, 15, and 20 k magnification levels. Figure 7 demonstrates that when particle size rose throughout the lyophilization process, the agglomeration phenomena intensified owing to the particles' smooth surfaces and spherical shapes. Studies using transmission electron microscopy (TEM) confirmed the nanometer-sized, almost spherical particles.

4.2.2 *In vitro* drug release study

Figures 8A and 8B show the *in vitro* drug release results for ranolazine loaded SLNs and drug solution in 0.1 N HCl (1% SLS) and PBS pH 6.8 (1% SLS). Because ranolazine is more soluble in acidic conditions, SLNs soaked in 0.1 N HCl (1% SLS) released more of the medication in 2 h (8.69 1.39%) than those soaked in PBS pH 6.8 (1% SLS). PBS pH 6.8 (1% SLS) from suspension released about 100% of the drug in 6 h, which was quicker, higher, and complete than drug released from SLNs formulation (Figure 4B). The sluggish release of ranolazine from 2 SLNs in the GI tract may be confirmed by the fact that drug release from the SLNs formulation was only 34.26 0.95% after 8 h and 68.54 2.86% after 24 h. Ranolazine's modest rate of release from SLNs suggested that, upon oral administration, the medication might be absorbed by enterocytes, which would be useful for producing the desired therapeutic effect.

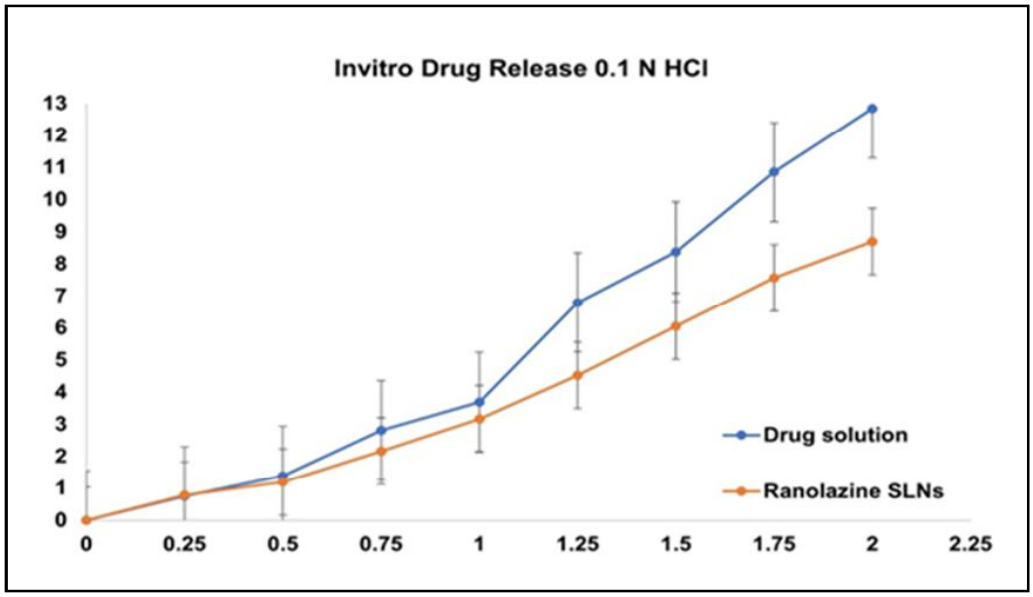

Figure 8 A: Optimization of ranolazine sustained-release nanoparticles and drug-solution *in vitro* drug-release studies.

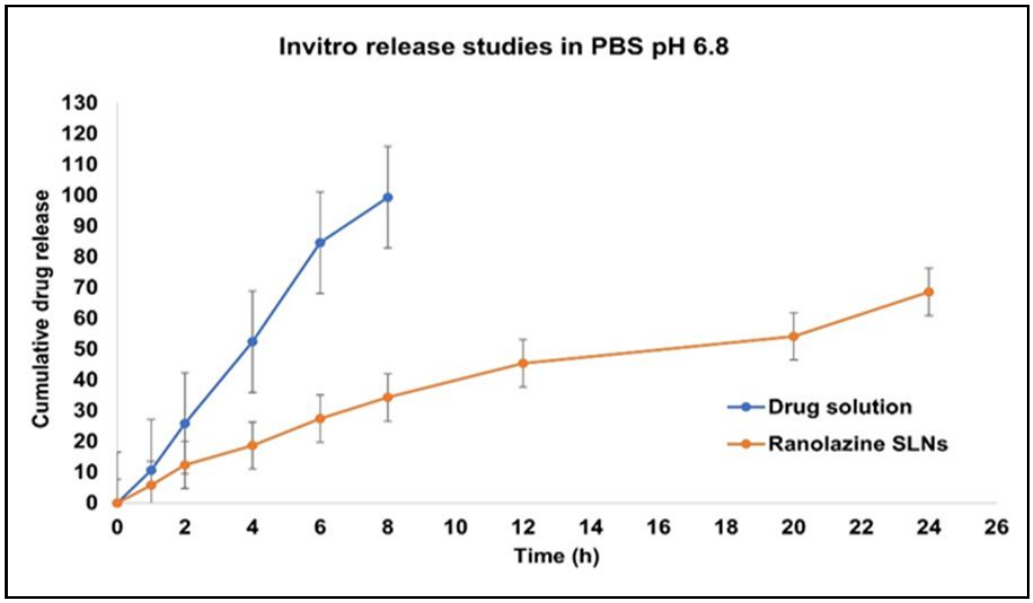

Figure 8 B: Optimization of ranolazine sustained-release nanoparticles and drug-solution *in vitro* drug-release studies.

4.2.3 *Ex vivo* drug diffusion study by using isolated rat's stomach and intestine

By graphing the cumulative % drug diffusion vs time, the results of the drug diffusion research in the stomach and in the intestine for both ranolazine solution and ranolazine loaded SLNS are graphically shown in Figure 9 and Figure 10. Based on a 10 h ex diffusion investigation, it was shown that after 2 h, only 4.86 0.67% of the drug diffused from the SLNs dispersion and 22.38 0.95% from the ranolazine solution in the case of stomach drug diffusion. After 8 h, drug diffusion from SLNs dispersion in the duodenum was only 43.562.35% and from ranolazine solution was 98.371.23%. For this experiment, we mimicked gastric emptying by monitoring rat stomach and duodenum activity for a total of 10 h. Researchers found that drug release from solid lipid nanoparticles was statistically (p<0.05) greater than from drug suspension. This may be because the medicine is kept from coming into touch with stomach acid by the lipid. Diffusion in the duodenum was gradual and steady.

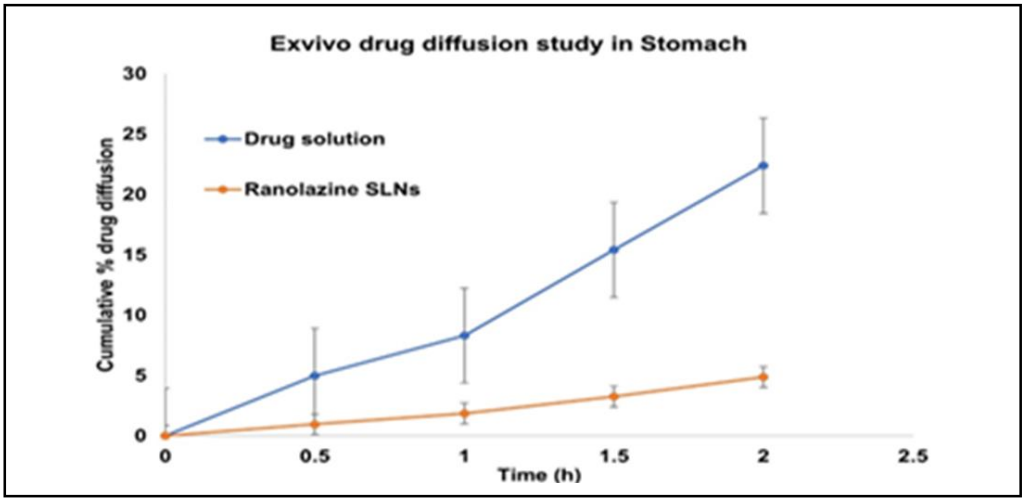

Figure 9 : ***Ex vivo*** **drug diffusion profile of drug solution and ranolazine loaded SLNs in stomach.**

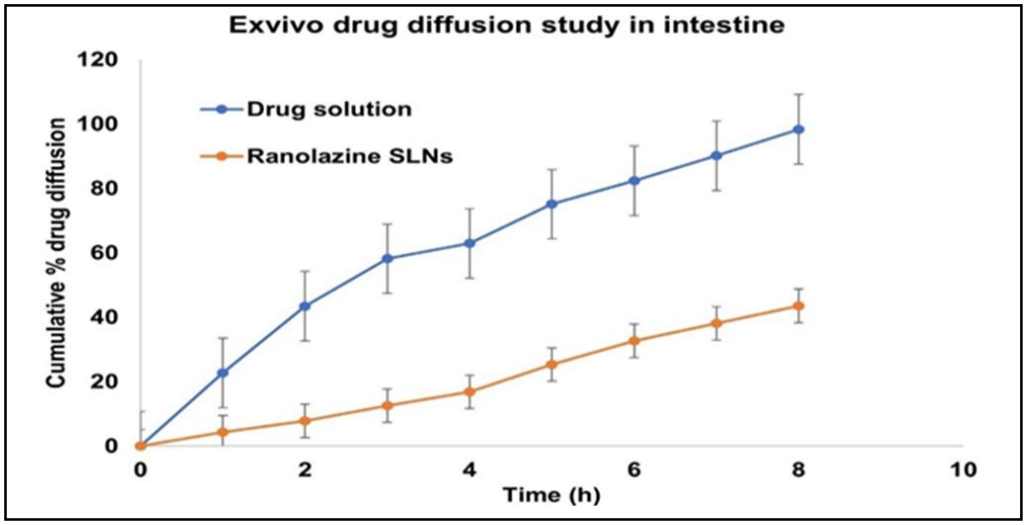

Figure 10 : ***Ex vivo*** **drug diffusion profile of drug solution and ranolazine loaded SLNs in the intestine.**

4.2.4 Lyophilization

SLNs powder was produced through freeze-drying the improved Ranolazine SLNs formulation, which included 10% maltose. Size, PDI, and zeta potential all increased after being reconstituted. When the attractive forces between particles would grow as the water was removed during the freeze-drying process (Sudha *et al*., 2020), this might explain why the SLNs formulation results in larger particles.

4.3 Pharmacokinetic study

Due to its limited water solubility, ranolazine has poor oral absorption. The first-pass effect is common with this medication. The potential of ranolazine nanosuspensions to boost the drug's oral bioavailability has been investigated. The purpose of this research was to see whether SLNs might be utilized to enhance ranolazine's oral distribution. By using non-compartmental estimates in Kinetica 2000 software, Version 5.0, Innaphase Corporation. Philadelphia, USA. The pharmacokinetic parameters of ranolazine in individual rats for optimum SLNs formulation and pure drug solution were computed. Pharmacokinetic characteristics such as area under the curve (AUC), maximum concentration (Cmax), minimum concentration (MRT), and half-life (t1/2) were determined for the

improved SLNs formulation and compared to those of the drug solution. Student paired *t*-test with an value of 0.01 was used for the statistical analysis in Graph Pad Graph Pad Prism (version 6.02. 2013, Graph Pad software, San Diego, CA, USA). Figure 11 displays the serum concentration versus time profiles after a single dosage of ranolazine-SLNs formulation and medication solution. All relevant pharmacokinetic parameters were determined and are shown in Table 3. Figure 11 shows that the Cmax for the SLNs formulation was significantly greater than that for the drug solution ($p<0.001$), coming in at 3.9460.11 g/ml vs 3.2184 0.28 g/ml. However, the peak concentration was reached in about the same amount of time as the control group. Overall absorption, as measured by area under the curve (AUC), was similarly greater for the SLNS formulation (84.706 56.95 g/ml.h) than for the drug solution (24.328 1.06 g/ml..h; $p<0.0001$). Due to a slower elimination rate, SLNs formulation of ranolazine resulted in a longer biological half-life and mean residence time. The oral bioavailability of SLNs formulation was found to be 3.48-fold higher than that of a drug solution. The improved bioavailability of ranolazine from SLNs formulations may be the result of many processes (Arjun *et al*., 2013), any one of which may have played a role alone or in concert. There are a few possible explanations for the increased rate of absorption caused by solid lipid nanoparticles (SLNs): I the SLNs are able to adhere to the GI tract and also to enter the interpillar spaces, thereby increasing the residence ti, because of their small size; (ii) the SLNs have a massive effective surface area due to their nano size; and (iii) the SLNs are able to enter the GI additionally, y) the presence of fatty acid favors lymphatic transport, with the effect being proportional to the chain length of the fatty acid used; the longer the chain, the greater the extent of lymphatic transport; and (v) surfactant's influence on the preferential uptake of lipid particles by Peyer's patches improves ranolazine's bioavailability by preventing first-pass metabolism. The findings suggest that SLNs may be useful as a carrier for increasing ranolazine's oral bioavailability.

Table 3: Pharmacokinetic parameters of ranolazine after oral administration of optimized SLNs formulation and drug solution (mean ± SD, n = 6).

Pharmacokinetics parameter	Drug solution	Ranolazine SLNs
Intercept	0.1128	0.1926
Slope	-0.0213	-0.0045
C0 (mcg/ml)	1.296	1.558127275
K(hr-1)	0.0491	0.0105
Dose (mg)	100	100
Vd (ml)	77112.495	64179.609
Vd (l)	77.112	64.179
t1/2 (h)	7.085	14.629
Clearance (l/h)	3.793	0.677
AUC 0-t (µg.h/ml)	0.449	0.514
AUC 1-t (µg.h/ml)	17.985	31.265
AUC t-inf (µg.h/mL)	5.894	116.48
AUC Total (µg.h/mL)	24.328 ± 1.39	84.706 ± 2.31
C max	3.218 ± 0.13	3.946 ± 3.95
T max	4.05 ± 0.11	4.19 ± 2.31
MRT	9.36 ± 0.23	22.51 ± 1.85

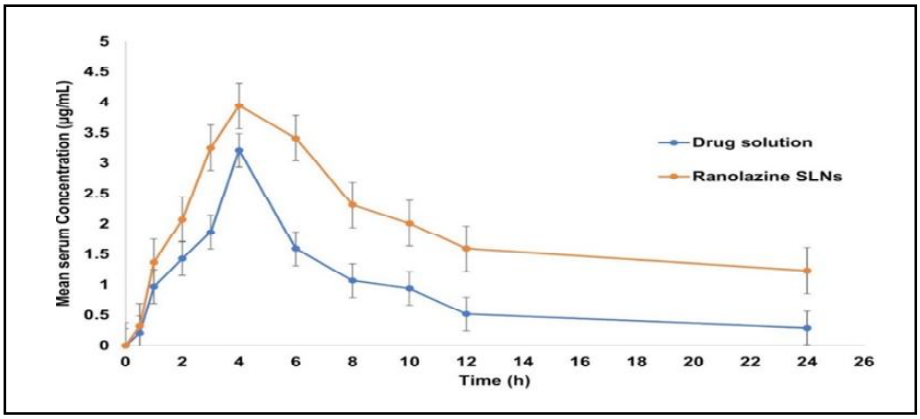

Figure 11: Ranolazine pharmacokinetics in rat serum after oral administration of an SLNs formulation and a medication solution (mean SD; n = 6).

4.4 Pharmacodynamic study

In a rat model of hypertension, the antihypertensive impact of SLNs formulation was compared to that of drug solution. Hypertension was generated in rats by giving them a 10% fructose solution by mouth. Instrumental (NIBP) measurement of systolic blood pressure; findings shown in Figure 12. Hypertension was initially considerably (p<0.05) reduced following oral administration of ranolazine solution, with maximal impact shown at 2 h. However, after 2 h, BP began progressively increasing and was back to baseline by 24 h. In contrast, after taking Ranolazinc-SLNs formulation orally, blood pressure gradually decreased, with the greatest impact shown at 24 h (p<0.05), with the effect lasting for 48 h. Up to 48 h after inducing hypertension with fructose, no reduction in systolic blood pressure was seen in the control group. Systolic blood pressure was also found to be normal in the control group of rats. Results from pharmacokinetic tests in rats showed that SLNS released the drug more slowly than a drug solution, with an AUC iotal, half-life, and MRT that were all more than twice as long. When administered ondly, rancluzine solution worked rapidly (2 h) and significantly, although its effects tapered down after 24 h, whereas the SLNs formulation was unable to significantly lower BP in the introductory phase, Ranolazine-SLNs induced a prolonged and steady drug release for at least 24 h after treatment. Accordingly, the hypertension was kept under control by the intended SLNs for a full 48 h. The limitations of oral administration of ranolazine, such as limited bioavailability and high first-pass metabolism, were clearly overcome by the developed SLNs formulation. Additionally, creating medications in SLNS formulation becomes a therapeutic benefit in managing hypertension slowly, gradually, and for long periods.

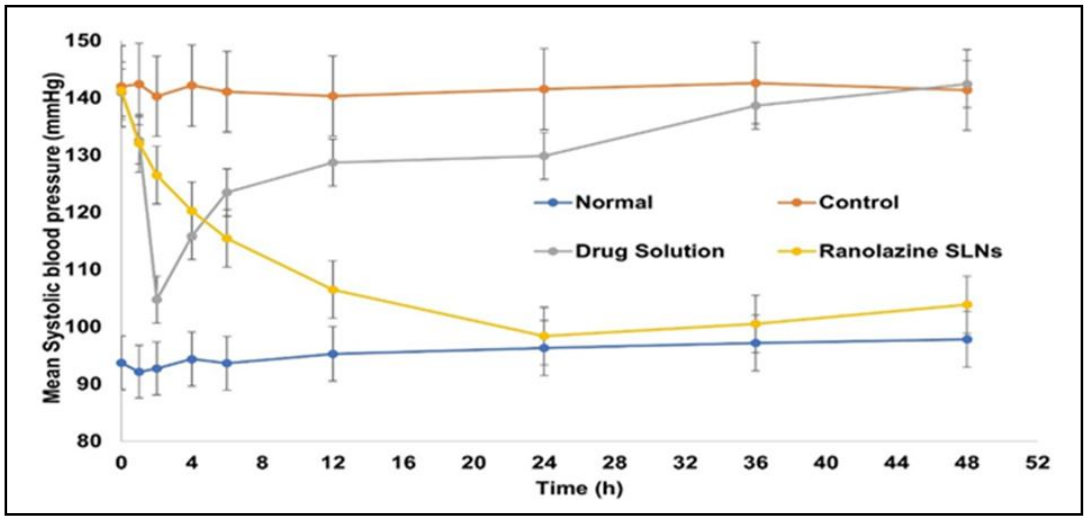

Figure 12: Orally administered ranolazine SLNs and medication solution on lowering blood pressure (mean SD, n = 6).

5. Stability studies

By comparing the appearance, particle size, PDI, ZP, assay, and entrapment efficiency of ranolazine before and after three months of storage in a refrigerator and at room temperature, we were able to confirm that the improved SLNs formulation was stable. When testing the SLNS formulation at set intervals, we saw no evidence of drug crystallization. The formulation's size, PDI, and ZP were measured to be in the following ranges: 0.0950.02 to 0.1350.12 at 4°C and 0.0950.02 to 0.2960.01 at 25°C; -22.52.07 to 26.411.34 mV at 4°C and -22.52.07 to -31.642.19 mV at 25°C. The results of the assay and EE showed values between 99.68 0.05 and 99.84 0.06 at 4°C, 88.34 1.2 and 81.69 0.25 at 25°C. and 88.34 12 and 86.29 0.06%. The particle size, PDI, and ZP of both the refrigerated and room-temperature storage samples did not significantly increase over the course of the three-month study period. The polymorphic shift of lipid matrix from metastable to stable form resulting in ejection of drug from the lipid matrix may account for ejection of drug from the lipid matrix may account for the substantially smaller size change seen in samples held at refrigerated temperature compared to those stored at room temperature (p>0.05).

6. Conclusion

Using a heat homogenization technique, primarily glyceryl monostearate and a 1:1 w/w ratio of Poloxamer 188: tween 80, stable ranolazine loaded SLNs were produced. The findings demonstrated that the ranolazine-loaded SLNs were stable, nanometer-sized spherical particles with reduced PDI and improved *in vitro* release in stimulated fluids. After oral administration of ranolazine-loaded SLNs in rats, the drug's plasma exposure increased by about 2.3-fold. Based on the findings, ranolazine-loaded SLNs may serve as a viable alternative to the standard treatment for hypertension by addressing the issues of poor solubility, limited oral absorption, and therefore lower bioavailability. Therefore, the new ranolazine-loaded SLNs may provide a more efficient and effective drug delivery strategy than the status quo in hypertension.

Acknowledgments

I fully acknowledge the staff and management of The Pharmaceutical College, Barpali, my guide, Prof. (Dr) B.C Behera and our Lab assistant Mr. RK Thait for their help and support for this work.

Conflict of interest

The authors declare no conflicts of interest relevant to this article.

References

Amarachinta, P.R.; Sharma, G. and Samed. (2021). Central composite design for the development of carvedilol-loaded transdermal ethosomal hydrogel for extended and enhanced anti-hypertensive effect. J. Nanobiotechnol, **19**:100.

Arjun, N. and Kishan, V. (2013). Preparation, characterization and evaluation of quetiapine fumarate solid lipid nanoparticles to improve the oral bioavailability. J. Pharma., **12**:21-31.

Ashok, K.P.; Chandrakant, G.B. and Krishnapriya, M. (2010). Bioanalytical method development and its validation for determination of candesartan cilexetil by high performance liquid chromatography with UV detection. Acta. Pharma Sci., **52**:247-253.

Attari, Z.; Bhandari, A.; Jagadish, P.C. and Lewis, S. (2016). Enhanced *ex vivo* intestinal absorption of olmesartanmedox omilnano suspension: Preparation by combinative technology. Saudi Pharmaceutical Journal, **24**(1):57-63.

Bhaskar, K.; Krishna, M.C. and Lingam, M. (2009). Development of SLN and NLC enriched hydrogels for transdermal delivery of nitrendipine: *In vitro* and *in vivo* Characteristics. Drug Dev. Ind. Pharm., **35**:98-113.

Carvalho, S.M.; Noronha, C.M.; Floriani, C.L.; Lino, R.C.; Rocha, G.; Bellettini, I.C.; Ogliari, P.J. and Barreto P.L. (2013). Optimization of α-tocopherol loaded solid lipid nanoparticles by central composite design. Industrial Crops and Products, **31**(49):278-285.

Cavalli, R.; Caputo, O. and Carlotti, M.E. (1997). Sterilization and freeze-drying of drug-free and drug-loaded solid lipid nanoparticles. Int. J. Pharm., **148**:47-54.

Chaitman, B.R.; Ivleva, A.Y.; Ujda, M.; Lenis. J.H.F.; Toth,C.; Stieber, C,M.; Reisin, J.H.F.; Pangerl, A.M.; Friedman, J.B. and Lawrence. (2005). Antianginal efficacy of omapatrilat in patients with chronic angina pectoris, Am. J. Cardiol., **96**:1283-1289.

ChettupalliA.K.,;Ananthula, M.,; Amarachinta, P.R.; Bakshi, V. and Yata, V.K. (2021). Design, Formulation, *in vitro* and *ex vivo* evaluation of atazanavir loaded cubosomal gel. Biointerface Res. Appl. Chem., **11**(4):12037-12054.

Dandamudi, S. P.; Chettupalli, A. K.; Dargakrishna, S. P.; Nerella, M.; Amara, R. R. and Yata,V. K. (2022). Response Surface Method for the Simultaneous Estimation of Atorvastatin and Olmesartan. Trends in Sciences, **19**(18):5799.

Delie, F. and Blanco-Príeto, M.J.(2005). Polymeric particulates to improve oral bioavailability of peptide drugs. Molecules, **10**:65-80.

Elsayed, M.M.; Abdallah, O.Y.; Naggar, V.F. and Khalafallah, N.M.;(2007). Lipid vesicles for skin delivery of drug: reviewing three decades of research, Int. J. Pharm., **332**:1-16.

Hwang, I.S.; Ho H.; Hoffman, B.B. and Reaven, G.M. (1987). Fructose-induced insulin resistance and hypertension in rats. Hypertension, **10**:512-516.

Imad Uddin, M.D.; Venkata, R.J.; PreethiKarunya, Y.; Chakraborty, R. and Deepika, R. (2020). Synthesis and characterization of chitosan nanoparticles loaded with 6-gingerol isolated from Zingiberofficinale rosc. Ann. Phytomed., **9**(2):164-171

Jun-Bo, T.; Y, Zhuang-Qun.; Xi-Jing, H.; Ying, X.; Yong, S.; Zhe, X. and Tao,C. (2007). Effect of ethosomalminoxidil on dermal delivery and hair cycle of C57BL/6 mice, J. Dermatol. Sci., **45**:135-137.

Kumar, T.S. and Chettupalli, A.K. (2018). Studies on statistically optimized binary ethosomal gel encapsulated with Carvedilol: *Ex vivo* permeation and pharmacodynamic assessment in male wistar albino rats. Mol2Net, 1(Section A, B, C, *etc*.). DOI:10.3390/mol2net-04-05563

Luo, Y.; Chen, D.; Ren, L.; Zhao, X. and Qin, J. (2006). Solid lipid nanoparticles for enhancing vinpocetine's oral bioavailability. J. Control Release, **114**:53-59.

Madhu, B.; Raju, J. and Karthik Y.J. (2013). Enhanced intestinal absorption and bioavailability of raloxifene hydrochloride *via* lyophilized solid lipid nanoparticles. Adv Powder Technol, **24**:393-402.

Manjunath, K. and Venkateswarlu V. (2005). Pharmacokinetics, tissue distribution and bioavailability of clozapine solid lipid nanoparticles after intravenous and intraduodenal administration. J. Contr Rel., **107**:215-228

Mehnert, W. and Mäder, K. (2001). Solid lipid nanoparticles production, characterization and applications. Adv. Drug Deliv Rev., **47**:165-196.

Mehnert, W. and Mäder K. (2012). Solid lipid nanoparticles production, characterization and applications. Adv. Drug Deliv Rev., **64**:83-101.

Paolino, D.; Lucania, G.; Mardente, D.; Alhaique, F. and Fresta, M. (2005) Ethosome for skin delivery of ammonium glycyrrhizinate: *In vitro* percutaneous permeation through human skin and *in vivo* anti-inflammatory activity on human volunteers, J. Contrl. Rel., **106**:99-110.

Parmar, B.; Mandal, S.; Petkar, K.C.; Patel, L.D. and Sawant, K.K. (2011). Valsartan loaded solid lipid nanoparticles: Development, characterization, and *in vitro* and *ex vivo* evaluation. Int. J. Pharm. Sci. Nanotechnol., **4**:1483-1490.

Pradhan, K.K.; Mishra, U.S. and Pattnaik, S. (2011). Development and validation of a stability-indicating UV spectroscopic method for candesartan in bulk and formulations. Ind. J. Pharm. Sci., **73**:693-696.

Priya, T.; Vaseem, A.A.; Tarique, M. and Farogh, A. (2022). Augmentation and evaluation of betasitosterol based liposomes. Ann. Phytomed., **11**(1): 648-656

Schwarz, C. (1999). Solid lipid nanoparticles (SLN) for controlled drug delivery II. Drug incorporation and physicochemical characterization. J. Microencapsul., **16**:205-213.

Schwarz, C.; Mehnert, W.; Lucks, J.S. and Müller, R.H.; (1994). Solid lipid nanoparticles (SLN) for controlled drug delivery-1. Production, characterization and sterilization. J. Contr Rel., 30:83-96

Smith, P.L.; (1996). Methods for evaluating intestinal permeability and metabolism *in vitro*. In Models for Assessing Drug Absorption and Metabolism¸ Springer US. pp:13-34.

Sudha,B.; Sumathi, S. and Swabna, V. (2020). Enzyme mediated synthesis and characterization of silver nanoparticles using keratinase enzyme producing micro-organisms. Ann. Phytomed., **9**(1): 147-153.

Tardif. J.C.; Ford, I.; Tendera, M. and Bourassa, M.G. (2005). Fox, For the Initiative Investigators. Efficacy of ivabradine, a new selective if inhibitor, compared with atenolol in patients with chronic stable angina, Eur. Heart. J., **26:**2529-2536.

Torsten, M.G. and Müller, R.H. (2005). Protein adsorption patterns on poloxamer-and poloxamine-stabilized solid lipid nanoparticles (SLN). Eur. J. Pharm. Biopharm., **60**:361-72.

Unnisa, A.; Chettupalli, A.K.; Al Hagbani, T.; Khalid, M.; Jandrajupalli, S.B.; Chandolu, S. and Hussain, T. (2022). Development of dapagliflozin solid Lipid nanoparticles as a novel carrier for oral delivery: Statistical Design, Optimization, *in vitro* and *in vivo* Characterization, and Evaluation. Pharmaceuticals, **15**:568.

Varshosaz, J.; Ghaffari, S.; Khoshayand, M.R.; Atyabi, F.; Azarmi, S. and Kobarfard, F. (2010). Development and optimization of solid lipid nanoparticles of amikacin by central composite design. Journal of Liposome Research., **20**(2):97-104.

Vasudha, B.; Rao, A.P. and Chettupalli, A.K. (2022). Design, development and optimization of solid lipid nanoparticles of Rizatriptan for intranasal delivery: *In vitro* and *in vivo* assessment, Materials Today: Proceedings, **66**(4):2342-2357.

Veerendra, C.Y.; Manjiri, A. R,; Yasmin, H. M. and Rajendra, C.D. (2021). Formulation, characterization and evaluation of in vitro antioxidant potential of melatonin and quercetin loaded liposomes. Ann. Phytomed., **10**(2): 327-334.

Vijay, N.K.; Raviraj, P.; Venkateshwarlu, V. and Harisudhan, T. (2009). Development and characterization of solid oral dosage form incorporating candesartan nanoparticles. Pharm. Dev. Tech., **14**:290-298.

Vinay, V.; Chandrasekhar, D. and Ramakrishna. (2007). Development and evaluation of nitrendipine loaded solid lipid nanoparticles: Influence of wax and glyceride lipids on plasma pharmacokinetics. Int. J. Pharm., **335**:167-175.

Weon, K.Y.; Lee, K.T. and Seo, S.H. (2000). Optimization study on the formulation of Roxithromycin dispersible tablet using experimental design. Archives of Pharmacal Research; **23**(5):507-512.

Citation **Abdul Sayeed Khan and Bhupen Chandra Behera (2022). Ranolazine loaded solid lipid nanoparticles for oral delivery: Characterization, pharmacokinetic and pharmacodynamic evaluation. Ann. Phytomed., 11(2):689-702. http://dx.doi.org/10.54085/ap.2022.11.2.85.**